Journal of Chromatography A, 1440 (2016) 31–36

Contents lists available at ScienceDirect

Journal of Chromatography A

journal homepage: www.elsevier.com/locate/chroma

Inverse supercritical fluid extraction as a sample preparation method for the analysis of the nanoparticle content in sunscreen agents

David Müller[a,b,*], Stefano Cattaneo[a], Florian Meier[c], Roland Welz[c], Tjerk de Vries[d], Meital Portugal-Cohen[e], Diana C. Antonio[f], Claudia Cascio[f], Luigi Calzolai[f], Douglas Gilliland[f], Andrew de Mello[b]

[a] Centre Suisse d'Electronique et de Microtechnique (CSEM), Bahnhofstrasse 1, 7302 Landquart, Switzerland
[b] Institute for Chemical and Bioengineering, Department for Chemistry and Applied Biosciences, ETH Zürich, Vladimir-Prelog-Weg 1, 8093 Zürich, Switzerland
[c] Postnova Analytics GmbH, Max-Planck-Str. 14, 86899 Landsberg am Lech, Germany
[d] Feyecon Carbon Dioxide Technologies, Rijnkade 17a, 1382 GS Weesp, The Netherlands
[e] AHAVA Dead Sea Laboratories, 1 Arava Street, 70150 Lod, Israel
[f] European Commission—Joint Research Centre, IHCP, via E. Fermi 2749 I, 21027 Ispra, VA, Italy

ARTICLE INFO

Article history:
Received 2 September 2015
Received in revised form 19 February 2016
Accepted 21 February 2016
Available online 26 February 2016

Keywords:
Sample preparation
Supercritical carbon dioxide
Nanoparticle separation
Inverse supercritical fluid extraction
Field flow fractionation

ABSTRACT

We demonstrate the use of inverse supercritical carbon dioxide ($scCO_2$) extraction as a novel method of sample preparation for the analysis of complex nanoparticle-containing samples, in our case a model sunscreen agent with titanium dioxide nanoparticles. The sample was prepared for analysis in a simplified process using a lab scale supercritical fluid extraction system. The residual material was easily dispersed in an aqueous solution and analyzed by Asymmetrical Flow Field-Flow Fractionation (AF4) hyphenated with UV- and Multi-Angle Light Scattering detection. The obtained results allowed an unambiguous determination of the presence of nanoparticles within the sample, with almost no background from the matrix itself, and showed that the size distribution of the nanoparticles is essentially maintained. These results are especially relevant in view of recently introduced regulatory requirements concerning the labeling of nanoparticle-containing products. The novel sample preparation method is potentially applicable to commercial sunscreens or other emulsion-based cosmetic products and has important ecological advantages over currently used sample preparation techniques involving organic solvents.

1. Introduction

Today, a growing number of consumer products make use of the unique physical and chemical properties of nanomaterials. As the number of such products increases, the ability to thoroughly characterize their properties and functionality becomes critical. In particular, the recent regulatory efforts concerning the labeling of nanoparticle-containing consumer products, e.g., the EU regulations on cosmetics [1] and food [2], call for the development of simple and robust sample preparation protocols enabling a reliable detection and quantification of nanoparticulate ingredients in complex matrices [3–5]. This problem is especially challenging in case of emulsion-based consumer products such as cosmetics, which often consist of complex multicomponent matrices [6]. Commercially available sunscreen formulations for example usually contain more than 20 ingredients with different functions and physicochemical properties. Moreover, such viscous samples cannot be directly injected into an analytical system, and need to be liquefied prior to analysis. Commonly applied sample preparation protocols include chemical treatments using organic solvents [7–11]. Such complex processes are both time-consuming and have a considerable environmental impact due to the extensive use of organic solvents of which many are ecologically harmful [12–14]. The generalization and simplification of sample preparation workflows, as well as the reduced usage of organic solvents, is therefore likely to have a significant impact on the utility of analyses of nanoparticle-containing samples.

To this end, we herein report the use of inverse supercritical fluid extraction (inverse SFE) [14–18], a more ecological and simpler sample preparation method based on the use of supercritical fluids. For our application we selected supercritical carbon dioxide

* Corresponding author at: Centre Suisse d'Electronique et de Microtechnique (CSEM), Bahnhofstrasse 1, 7302 Landquart, Switzerland. Fax: +41 81 307 81 00.
E-mail address: david.mueller@csem.ch (D. Müller).

http://dx.doi.org/10.1016/j.chroma.2016.02.060
0021-9673/

($scCO_2$), as many of the chemical excipients found in large numbers in emulsion-based cosmetic products are of a fatty and non-polar nature and therefore exhibit a high solubility in CO_2. Furthermore, $scCO_2$ is chemically inert [18], nontoxic, nonflammable [19], and it is well-known for its application in SFE processes, where it is commonly used to extract small and/or non-polar molecules from natural materials under very mild conditions [20–23]. Besides the extraction of essential oils from herbs and spices [24,25], the most prominent application of SFE is the removal of caffeine from coffee beans [26,27]. The process has also been employed for the extraction and analysis of antioxidants, preservatives and sunscreen agents in cosmetics [28,29]. In these applications, however, the SFE is used to dissolve and extract the analyte from the matrix. In this work, inverse SFE is used as a sample treatment to simplify the matrix by removing unwanted components, thus keeping the target nanomaterials in the residual sample. Inverse SFE has also been studied for over twenty years. To date, it has primarily been used for the isolation of non-polar pharmaceutical formulations from polar analytes [14,16,17] and not for the pre-treatment of nanoparticle-containing samples. The minimal surface tension, low viscosities and gas-like diffusivities of $scCO_2$ allow for thorough sample penetration whilst maintaining the structure of the residual material [14]. Once the sample treatment is completed, the CO_2 is simply removed by lowering the pressure to below the critical threshold and returning to ambient conditions. The remaining material consists of the polar components (thickening agents) along with the nanoparticles that accordingly, can easily be rewet and subsequent dispersed in a direct manner. To demonstrate the potential utility of such a sample preparation process in the analysis of nanoparticle containing sunscreens, we integrated the $scCO_2$ treatment with Asymmetrical Flow Field-Flow Fractionation (AF4) hyphenated with UV and Multi-Angle Light Scattering (MALS) detection, and tested the method with a model sunscreen sample. The obtained findings were verified by Scanning Transmission Electron Microscopy (STEM) and Energy-Dispersive X-ray (EDX) analysis. Although the method is demonstrated using a model sunscreen matrix, we expect it to be applicable to commercial sunscreens or other emulsion-based cosmetic products, which include fatty additives with a high solubility in $scCO_2$.

2. Materials and methods

2.1. Chemicals

2.1.1. Titanium dioxide nanoparticle samples

A titanium dioxide (TiO_2)—nanoparticle dispersion, AERODISP® W 740 X (40% w/w, EVONIK Industries, Hanau, Germany) was diluted with ultrapure water (MilliQ, Billerica, USA). This was followed by addition of 0.2% (v/v) NovaChem (Postnova Analytics GmbH, Landsberg, Germany) to yield a final particle concentration of 0.2 mg/mL. NovaChem is a mixture of non-ionic and ionic detergents that helps to prevent particle agglomeration. Prior to analysis, the sample was placed in an ultrasonic bath (Sonorex Digital 10 P, Bandelin, Berlin, Germany) and sonicated at maximum power (320 W, 35 kHz) for 30 min to further reduce eventual particle agglomerates.

2.1.2. Model sunscreens

The novel sample preparation method was tested on two complex sunscreen model samples, one with and one without nanoparticles. The creams were produced separately, although both consisted of the following excipients: Avicel® PC611 (FMC Biopolymer, Brussels, Belgium), glycerin (Thai Oleochemicals Ltd., Bangkok, Thailand), KELTROL® T (Bronson & Jacobs Pty Ltd., Villawood, NSW, Australia), potassium sorbate (APAC Chemical Corp., Arcadia, CA, USA) and ultrapure water (MilliQ, Billerica, USA) in the water phase and Antaron™ V216 (ISP Ltd., Tadworth, UK), Arlacel™ 165 (JEEN, Fairfield, NJ, USA), capric/caprilic triglycerine (HENKEL KGaA, Düsseldorf, Germany), cyclomethiocone (Momentive Amer Ind., Waterford, NY, USA), Emulsiphos® (Symrise, Holzminden, Germany), isostearyl isostearate (UNIQEMA Corp., New Castle, DE, USA), octyl palmitate (Eigenmann & Veronelli, Milano, Italy), stearyl alcohol (Temix International, Milano, Italy), TEGO® Care 450 (EVONIK Industries, Essen, Germany), Finsolv® TN (Innospec, Englewood, CO, USA) and tocopheryl acetate (BASF SE, Ludwigshafen, Germany) in the oil phase. Both phases were mixed independently for 15 min using a L4R Mixer (Silverson Machines Inc., East Longmeadow, MA, USA) at 6000 rpm before they were homogenized together for another 15 min using again the L4R at 6000 rpm. In the last step, Dow Corning® 1503 (Dow Corning Corporation, Midland, MI, USA), Euxyl® PE 9010 (Schülke & Mayr GmbH, Norderstedt, Germany) and 12.5% w/w of a AERODISP® W 740 X TiO_2 nanoparticle dispersion (40% w/w, EVONIK Industries, Essen, Germany) were added to one cream, resulting in a TiO_2 particle concentration of 5.0% w/w, a concentration typically found in commercial sunscreens [9,30]. In the blank cream, the AERODISP® nanoparticles were replaced with corresponding amounts of ultrapure water (MilliQ, Billerica, USA). Both creams were homogenized again for 5 min at 4000 rpm, before they were filled into tubes and stored at room temperature.

2.2. Sample treatment

2.2.1. Extraction equipment

Extraction was performed using a lab scale supercritical fluid extraction system (Lab SFE 100 mL, Separex, Champigneulles, France). The system was equipped with a high-pressure CO_2 pump, a pressure/flow regulating system, and a horizontally mounted 100 mL extraction vessel housed in a thermostated oven.

2.2.2. Supercritical CO_2 sample treatment

The model sunscreen (Fig. 1A) was placed on a Teflon cartridge surrounded by a stainless steel holder (Fig. 1B). The Teflon part contained a small recess resulting in a cavity with dimensions of $60 \times 10 \times 0.2$ mm. To ensure that a reproducible sample volume was assayed, excess sunscreen was removed each time using a spatula. The Teflon cartridge was then removed from its holder (Fig. 1C) and placed in the extraction vessel (100 mL, Separex, Champigneulles, France). The sample was then subjected to a constant $scCO_2$ flow of 100 g/min for 30 min at 40 °C and 131 bars. The optimum parameters were selected by performing a series of measurements with varying processing times, temperatures and pressures. Less aggressive conditions (such as shorter processing times, lower temperatures and lower pressures) resulted in reduced extraction efficiencies of the fatty components, leading to reduced solubility in water, whilst harsher conditions led to more extensive particle aggregation and reduced reproducibility. The treated sample (Fig. 1D) was then removed from the cartridge (Fig. 1E) and dissolved in ultrapure water (MilliQ, Billerica, USA), to which 0.2% (v/v) NovaChem (Postnova Analytics GmbH, Landsberg am Lech, Germany) was added until a concentration of less than 0.2 mg TiO_2 (related to a recovery of 100%) per mL of solvent (Fig. 1F). Sample dilution is necessary to prevent overloading effects, which cause peak shifts and further advanced particle aggregation. Extractions for both creams (with and without nanoparticles) were performed in triplicate.

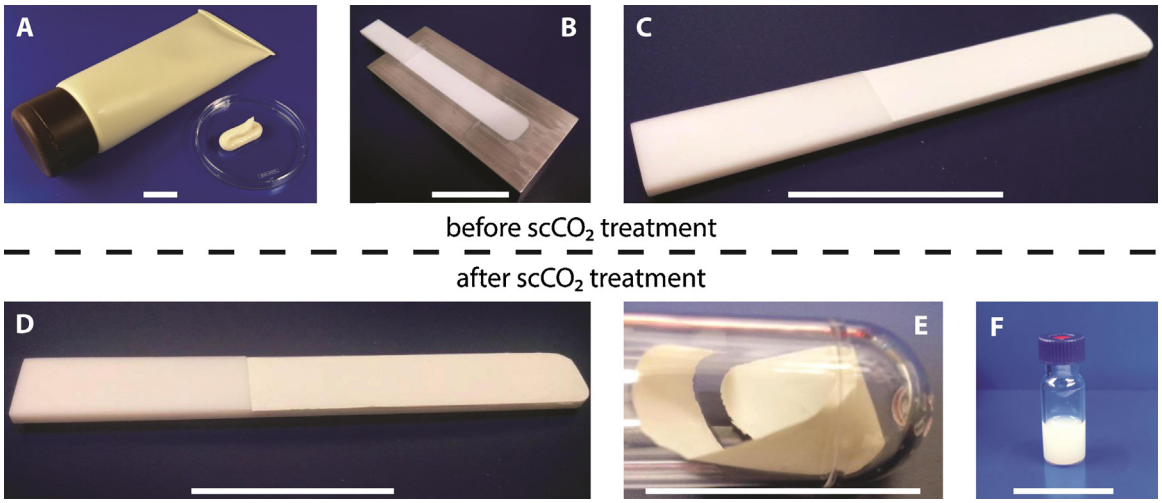

Fig 1. Model sunscreen at different stages before (A–C) and after (D–F) the supercritical CO_2 treatment. Scale bars are 25 mm. (A) The cream after being freshly dispensed from the tube. (B) Cream after deposition on the Teflon cartridge, held within the stainless steel holder. Excess cream is removed with a spatula to ensure a reproducible sample amount. (C) Teflon cartridge after being removed from the holder. The left side shows the handle of the cartridge, while the right (slightly shinier) side is the untreated, deposited cream. (D) After being processed by supercritical CO_2, the residual material has a darker, slightly beige color. (E) The sample is scraped off from the cartridge and stored in a plastic tube. (F) Before being processed by hyphenated AF4-UV-MALS, the residual material is re-dispersed in 0.2% NovaChem solution.

2.3. Multi-detector asymmetrical flow field-flow fractionation

2.3.1. Instrumentation and carrier liquid

Sunscreen samples were analyzed using a commercially available AF4 system (AF2000 MF, Postnova Analytics GmbH (PN), Landsberg am Lech, Germany) incorporating an autosampler (PN5300), channel thermostat (PN4020), UV (PN3211) and Multi-Angle Light Scattering MALS (PN3621, 21 angles) detectors. The storage temperature in the autosampler was set to 4 °C and the channel thermostat was set to 25 °C. UV detection was performed at 254 nm and the MALS detector provided the gyration radius of the particles exiting the AF4 separation cartridge (calculated with random coil model). The eluent was prepared using filtrated ultrapure water (MilliQ, Billerica, USA), to which 0.2% (v/v) filtered NovaChem (Postnova Analytics GmbH, Landsberg am Lech, Germany) was added. An analytical AF4 cartridge (S-AF4-CHA-611) incorporating a 10 kDa regenerated cellulose membrane (Z-AF4_MM-612-10KD) and a 350 μm thick Mylar spacer was used for all measurements and the injection volume was always set to 20 μl. Separations and analysis were performed in triplicates for each of the sample. In order to compensate the baseline drifts, the UV data was corrected by subtracting a blank run signal measured after an injection of pure eluent. Data acquisition and MALS calculations were performed using the AF2000 Control Unit software (Postnova Analytics GmbH, Landsberg am Lech, Germany) and further evaluations (such as curve normalization) were performed using OriginPro 2015 (OriginLab Corporation, USA).

2.3.2. Elution profile

An optimized focusing and elution method was developed to ensure reproducible analysis. The focusing step of the selected elution profile was commenced with a 7 min long injection flow of 0.2 mL/min and with a cross-flow of 1.4 mL/min. After a 30 s long transition time, elution started with a constant cross-flow of 1.4 mL/min for an additional 5 min, followed by an exponentially decreasing crossflow (exponent: 0.2), reaching a final value of 0.1 mL/min after 40 min, which was then maintained for 25 min. To ensure a stable signal, the detector flow rate was maintained at 0.5 mL/min, with the other flows adjusted accordingly.

2.3.3. Recovery rate and limit of detection/quantification

In addition to the size determination by MALS, quantitative data about the recovery of TiO_2 was gathered by measuring the area under the curve of the UV detector signal. With eight injections of different amounts of the pure AERODISP® dispersion over 1.5 orders of magnitude, a value of 642.0 A.U. per μg TiO_2 was determined (intercept: 0.58 (SE: 1.20), Slope: 642.01 (SE: 9.89), adj. R^2 of 0.998). To further focus on nanoparticulate TiO_2 and particles in the smaller sub-micron regime, a time range of 15–50 min of elution time was selected, corresponding to particles having their radius of gyration roughly between 20 and 160 nm. For the pure AERODISP® dispersion only 89.4 ± 3.6% (n = 3) of its content was measured in that time frame. This results in an expected signal of 574.0 ± 23.2 A.U. for this time frame per injected μg of TiO_2.

To only measure the TiO_2-related UV-absorption of our samples, a blank run with pure eluent was subtracted from the AERODISP® run, whereas the separation of a nanoparticle-free sunscreen was subtracted from the runs with the nanoparticle-containing sunscreens. The recovery rate was then calculated based on the expected absorption corresponding to the amount of sunscreen originally deposited on the Teflon cartridge.

Determination of the signal-to-noise (S/N-) ratio was performed by comparing measured signals from the nanoparticle-containing sunscreens with those of nanoparticle-free cream samples (blank eluent runs were subtracted from both) and establishing the minimum concentration at which the analyte can be reliably detected. To mainly focus on nanoparticulate TiO_2, a fraction with an elution time between 15 and 35 min was selected, corresponding to particles having their radius of gyration roughly between 20 and 60 nm. A S/N-ratio of 3 is used for the limit of detection (LOD) and a S/N-ratio of 10 is used for the limit of quantification (LOQ).

2.4. Electron microscopy

A droplet of sample was deposited on a copper grid covered by a thin carbon layer. The pure nanoparticle dispersion was then observed using a Transmission Electron Microscope (CM200 TEM, Philips, Eindhoven, The Netherlands). The $scCO_2$ treated samples were further analyzed with a Scanning Electron Transmission Microscope (Talos F200X, FEI, Hillsboro, OR, USA) equipped

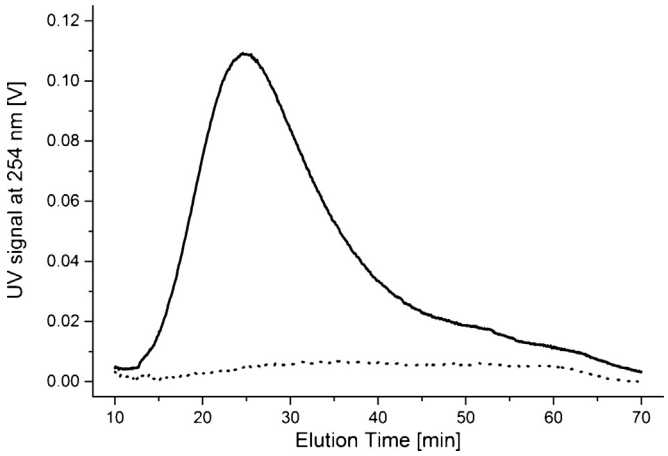

Fig. 2. Elugrams of the model sunscreens with and without nanoparticles. The black solid line reports the analysis of the re-suspension of the $scCO_2$ treated sample with 5% TiO_2 nanoparticles. A wide peak, indicating particles with a broad size distribution and hence eluting over an extended separation period, is evident. For the nanoparticle-free sample (black dotted line, also treated with $scCO_2$), no significant signal is detected over the complete separation cycle.

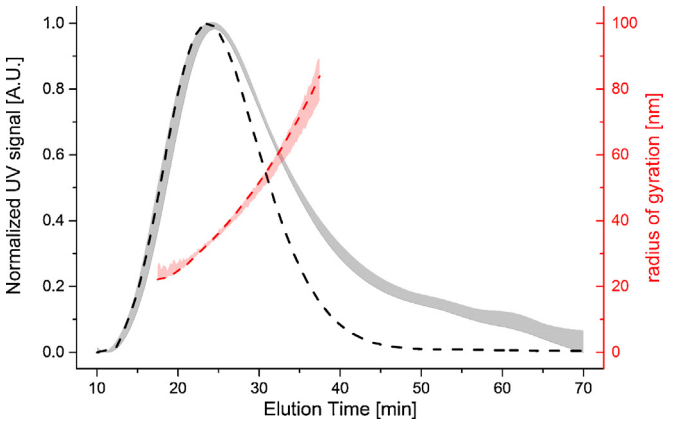

Fig. 3. UV curves (black) and MALS measurements (red) of the pure nanoparticle dispersion and the $scCO_2$ processed model sunscreen with nanoparticles. For both measurements, the dashed lines represent the data from pure AERODISP® dispersion, whereas the data from triplicate measurements of the $scCO_2$ treated samples are combined in a band. The UV signal of the AERODISP® nanoparticle dispersion elutes slightly earlier and with a narrower peak profile than the $scCO_2$-treated counterparts. Besides this, the main difference between the measurements is the presence of large agglomerates in the treated samples, having gyration radii in the range of several hundred nanometers (mainly between 40 and 60 min). Such agglomerates might occur during the sample pre-treatment or during one of the preceding steps in the sample life cycle.

with an X-FEG and a Super-X EDS system for spectroscopic mapping.

3. Results and discussion

3.1. Hyphenated AF4-UV-MALS measurement

After sonication, the re-dispersed samples were directly injected into the AF4 system. As shown in Fig. 2, the resulting UV curve allows an unambiguous distinction between the cream that contains nanoparticles (solid black line) and the nanoparticle-free sample (dotted black line). To investigate whether the sample preparation method induces a change in the size distribution of the nanoparticles, we compared the elugram and MALS data from a diluted dispersion of the pure AERODISP® nanoparticles to those obtained from the cream with nanoparticles after $scCO_2$ treatment and resuspension. To remove possible matrix effects, the UV signal of the $scCO_2$ treated blank cream was subtracted from that of the spiked cream. The resulting comparison (Fig. 3) shows that the original nanoparticle dispersion (dashed black line) elutes slightly earlier and with a narrower peak profile than the $scCO_2$-treated counterparts (gray band). At peak-maximum of the UV curve, this corresponded to an increase in radius of gyration from 32.9 nm (SD: 0.3 nm) in the pure dispersion to 34.0 nm (SD: 1.2 nm) in the $scCO_2$-treated model cream. Beside the slight shift of the UV peak, the main difference between the signal of the treated and the untreated nanoparticles are some large agglomerates with gyration radii in the range of several hundred nanometers (mainly between 40 and 60 min), that were observed in the $scCO_2$-treated sample only. It is known that the presence of organic acids can diminish the suspension stability of TiO_2 nanoparticles [31] and that such acids can be formed in the presence of water and $scCO_2$ [32]. However, it is also possible that the agglomeration occurred during one of the preceding steps in the sample life cycle (manufacturing/homogenization or storage) and is not necessarily due to the $scCO_2$ sample treatment. The particle radii of gyration extracted from the MALS measurements of the three $scCO_2$ treated samples are all within the red band in Fig. 3 and, considering the expected measurement uncertainty, are consistent with the data from the pure AERODISP® nanoparticles (red dashed line). This confirms that the $scCO_2$ treatment does not have a significant impact on the overall relationship between size and elution time, indicating that the interaction between the particles and the membrane/eluent has not been significantly altered.

3.2. Electron microscopy and particle analysis

To confirm that the detected signal in the processed model sunscreen originates from titanium dioxide nanoparticles, a sample fraction (taken at the maximum of the UV-peak) was further investigated using Transmission Electron Microscopy (TEM). Fig. 4A shows titanium dioxide nanoparticles from a diluted AERODISP® W 740 X TiO_2 dispersion. The nanoparticles have a distinct, particle-like morphology with a relatively broad size distribution consistent with the data obtained from MALS. The contrast between the particles and the amorphous carbon sample grid is strong and allows for easy imaging using classical TEM. The nanoparticles that remain after the $scCO_2$ sample treatment however could not be imaged with classical TEM, likely due to remaining water-soluble cream-components significantly decreasing the overall contrast. Using an Energy-Dispersive X-ray (EDX) detector, we specifically mapped the sample for the spectroscopic signal of titanium (Fig. 4B). Further mapping for the oxygen content resulted in an overlapping signal (Fig. 4C), confirming the presence of TiO_2. While the titanium mapping shows a distinctive particle boundary, the oxygen signal appears to be more diffuse, extending beyond the particles. This may partially originate from polar organic materials in the cream that remain after the $scCO_2$ extraction process. However, the main contribution to this background signal in the oxygen map is caused by the thin carbon-layer of the TEM grid, which is slightly oxidizing under ambient air conditions. This is a known contamination that cannot be prevented in a simple manner. To retrieve the morphological form of the $scCO_2$-treated particles, a High-Angle Annular Dark-Field (HAADF) detector was used, which is especially sensitive towards elements with a high atomic number. Employing this detector with the Scanning Transmission Electron Microscope (STEM) for imaging, the particles could be imaged as shown in Fig. 4D. An overlay of both EDX-maps and the HAADF-image (Fig. 4E) therefore confirmed that the particles detected in the processed sunscreen are indeed titanium dioxide nanoparticles,

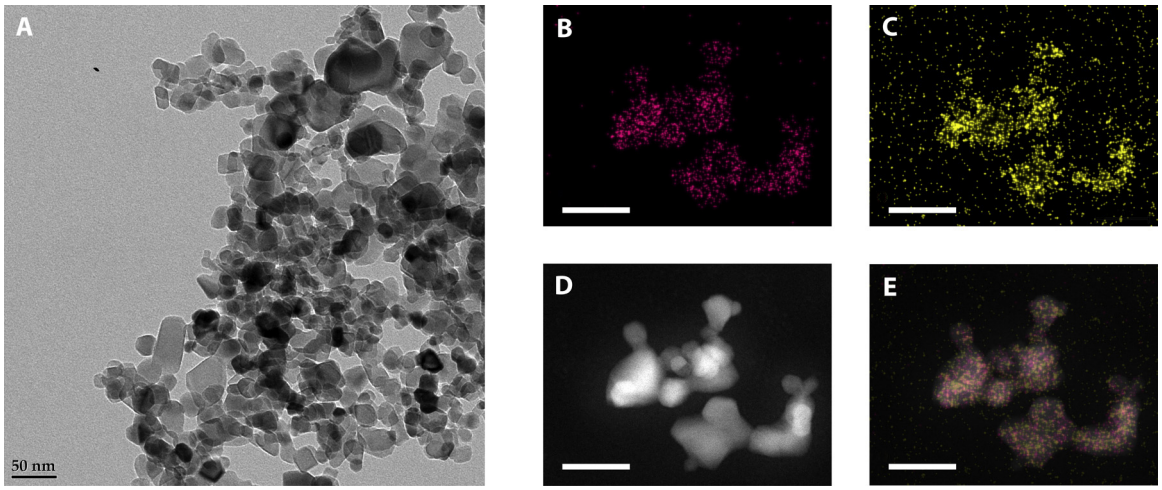

Fig. 4. Transmission electron microscopy images of the untreated suspension (A) and STEM-EDX chemical mapping as well as HAADF images of the $scCO_2$-treated TiO_2 nanoparticles (B–E). Scale bars are 50 nm. (A) TEM micrograph of the diluted AERODISP® dispersion, indicating a broad particle size distribution. The STEM-EDX maps show the elemental content of (B) titanium and (C) oxygen. (D) STEM image of the $scCO_2$-treated nanoparticles, taken with a high-angle annular dark field (HAADF) detector. (E) Overlay of the STEM-EDX maps of oxygen and titanium with the STEM-HAADF image of the same section. The precise overlay clearly demonstrates that the nanoparticles are indeed titanium dioxide nanoparticles. The main contribution to the background signal in the oxygen map is caused by the thin carbon-layer of the TEM grid, which is slightly oxidizing under ambient air conditions.

and that their morphological structure is preserved throughout the analytical procedure.

3.3. Recovery rate and limit of detection/quantification

For the evaluation of the recovery rate, the eluting TiO_2 of the three $scCO_2$-treated samples with nanoparticles was quantified using the conditions described in the materials and methods. The percentage recovery based on the mass of cream deposited on the cartridge, the dilution of the sample during resuspension and the total injection amount at the separation, was calculated. Recoveries ($n = 3$) of the three samples were $51.2 \pm 2.1\%$, $48.0 \pm 2\%$, and $52.2 \pm 2.3\%$, resulting in an overall recovery of $50.2 \pm 4.2\%$.This certainly leaves room for improvement, but is also significantly higher than what has been previously reported, e.g. for the extraction with organic solvents and tip sonication (8.14–21.47% in case of Ref. [9]).

The LOD for a single injection of 20 μL was found to be 0.6 μg of TiO_2 (30 μg/mL), corresponding to a LOQ of 2.0 μg (0.1 mg/mL). The latter approximately corresponds to a TiO_2 content of 0.5% (w/w) in the original sunscreen. These limits are well below the TiO_2 concentrations typically used in commercial sunscreen samples [9,30].

4. Conclusions

Prior research has demonstrated a variety of different sample pre-treatment methods for sunscreens and other consumer products containing nanoparticles, which are used to prepare them for subsequent analysis of the nanoparticle characteristics. Regrettably, most of these techniques suffer from the need to involve several working steps, which may impact the accuracy of the nanoparticle analysis. Furthermore, these techniques use large amounts of commonly aggressive and expensive chemicals, which have consequences for both operator safety and environmental sustainability.

In this work, we have presented a sample preparation method based on an inverse supercritical fluid extraction treatment that can be executed in a simple manner, and where the safe and non-toxic properties of CO_2 result in the elimination of ecological drawbacks, health hazards and associated disposal costs [14]. After treatment, the residual material can be easily re-dispersed in an aqueous solution and directly analyzed. Using AF4-UV-MALS, we confirmed the applicability of the $scCO_2$ method for the analysis of multicomponent and fatty samples in order to determine their nanoparticle content. The measurements were verified by STEM and EDX analysis. The results demonstrated that the presence of nanoparticles in a model sunscreen can be precisely determined, that a good recovery rate of roughly 50% of the particles of interest can be achieved and that the size distribution of those nanoparticles is essentially maintained. Compared to the original nanoparticle dispersion, an increase in larger particles/agglomerates was observed in the $scCO_2$-treated samples. This slight agglomeration might be caused by the sample treatment itself, but might also have occurred previously, e.g., during homogenization or storage. Overall, however, the size and morphology of the treated nanomaterials are found to be very similar to the original suspension, which is especially relevant in view of the recent regulatory requirements for nanoparticle containing cosmetics. Although the method is demonstrated using a model sunscreen matrix, we expect it to be applicable to commercial sunscreens or other emulsion-based cosmetic products.

Acknowledgments

This work was supported by the European Commission 7th Framework Programme (project SMART-NANO, NMP4-SE-2012-280779). Furthermore, the authors acknowledge the support of the Scientific Center for Optical and Electron Microscopy (ScopeM) at the Swiss Federal Institute of Technology ETHZ.

References

[1] EC, REGULATION (EC) No 1223/2009 on cosmetic products, Off. J. Eur. Union. (2009) 59–209.
[2] EC, REGULATION (EU) No 1169/2011 on the provision of food information to consumers, Off. J. Eur. Union. (2011) 18–63.
[3] A. Ulrich, S. Losert, N. Bendixen, A. Al-Kattan, H. Hagendorfer, B. Nowack, et al., Critical aspects of sample handling for direct nanoparticle analysis and analytical challenges using asymmetric field flow fractionation in a multi-detector approach, J. Anal. At. Spectrom. 27 (2012) 1120, http://dx.doi.org/10.1039/c2ja30024a.
[4] K. Loeschner, J. Navratilova, C. Købler, K. Mølhave, S. Wagner, F. Von Der Kammer, et al., Detection and characterization of silver nanoparticles in chicken meat by asymmetric flow field flow fractionation with detection by conventional or single particle ICP-MS, Anal. Bioanal. Chem. 405 (2013) 8185–8195, http://dx.doi.org/10.1007/s00216-013-7228-z.
[5] S. Wagner, S. Legros, K. Loeschner, J. Liu, J. Navratilova, R. Grombe, et al., First steps towards a generic sample preparation scheme for inorganic engineered

nanoparticles in a complex matrix for detection, characterization, and quantification by asymmetric flow-field flow fractionation coupled to multi-angle light scattering and, J. Anal. At. Spectrom. 00 (2015) 1–11, http://dx.doi.org/10.1039/C4JA00471J.
[6] L. Calzolai, D. Gilliland, F. Rossi, Measuring nanoparticles size distribution in food and consumer products: a review, Food Addit. Contam. Part A 29 (2012) 1183–1193, http://dx.doi.org/10.1080/19440049.2012.689777.
[7] C. Contado, A. Pagnoni, TiO_2 nano- and micro-particles in commercial foundation creams: field flow-fractionation techniques together with ICP-AES and SQW voltammetry for their characterization, Anal. Methods 2 (2010) 1112–1124, http://dx.doi.org/10.1039/c0ay00205d.
[8] A. Samontha, J. Shiowatana, A. Siripinyanond, Particle size characterization of titanium dioxide in sunscreen products using sedimentation field-flow fractionation-inductively coupled plasma-mass spectrometry, Anal. Bioanal. Chem. 399 (2011) 973–978, http://dx.doi.org/10.1007/s00216-010-4298-z.
[9] C. Contado, A. Pagnoni, TiO_2 in commercial sunscreen lotion: flow field-flow fractionation and ICP-AES together for size analysis, Anal. Chem. 80 (2008) 7594–7608, http://dx.doi.org/10.1021/ac8012626.
[10] R. Dunford, A. Salinaro, L. Cai, N. Serpone, S. Horikoshi, H. Hidaka, et al., Chemical oxidation and DNA damage catalysed by inorganic sunscreen ingredients, FEBS Lett. 418 (1997) 87–90, http://dx.doi.org/10.1016/S0014-5793(97) 01356-2.
[11] Z. a. Lewicka, A.F. Benedetto, D.N. Benoit, W.W. Yu, J.D. Fortner, V.L. Colvin, The structure, composition, and dimensions of TiO_2 and ZnO nanomaterials in commercial sunscreens, J. Nanopart. Res. 13 (2011) 3607–3617, http://dx.doi.org/10.1007/s11051-011-0438-4.
[12] C. Capello, U. Fischer, K. Hungerbu, What is a green solvent? A comprehensive framework for the environmental assessment of solvents, Green Chem. 9 (2007) 927–934, http://dx.doi.org/10.1039/b617536h.
[13] J.O. Metzger, Solvent-Free Organic Syntheses, Angew. Chem. Int. Ed. Engl. 37 (1998) 2975–2978.
[14] W.N. Moore, L.T. Taylor, Analytical inverse supercritical fluid extraction of polar pharmaceutical compounds from cream and ointment matrices, J. Pharm. Biomed. Anal. 12 (1994) 1227–1232.
[15] A.L. Howard, M.C. Shah, P. Ip, A. Brooks, J. Thompson, T. Taylor, Use of Supercritical fluid extraction for sample preparation of sustained-release felodipine tablets, J. Pharm. Sci. 83 (11) (1994) 1537–1542.
[16] D.C. Messer, L.T. Taylor, Inverse analytical supercritical fluid extraction of zovirax ointment 5%, Anal. Chem. 66 (1994) 1591–1592.
[17] R.A. Almodo, R.A. Rodrı, Inverse supercritical extraction of acetaminophen from suppositories, J. Pharm. Biomed. Anal. 17 (1998) 89–93.
[18] S. Scalia, S. Simeoni, Assay of xanthene dyes in lipsticks by inverse supercritical fluid extraction and HPLC, Chromatographia 53 (2001) 490–494.
[19] G. Kaupp, Reactions in supercritical carbon dioxide, Angew. Chem. Int. Ed. Engl. 33 (1994) 1452–1455.
[20] D.P. Ndiomu, C.F. Simpson, Some applications of supercritical fluid extraction, Anal. Chim. Acta. 213 (1988) 237–243.
[21] S.B. Hawthorne, Analytical-scale supercritical fluid extraction, Anal. Chem. 62 (1990) 633–642.
[22] H. Engelhardt, J. Zapp, P. Kolla, Sample preparation by supercritical fluid extraction in environmental food and polymer analysis, Chromatographia 32 (1991) 527–537.
[23] E. Reverchon, I. De Marco, Supercritical fluid extraction and fractionation of natural matter, J. Supercrit. Fluids. 38 (2006) 146–166, http://dx.doi.org/10.1016/j.supflu.2006.03.020.
[24] M. Goto, M. Sato, T. Hirose, Extraction of peppermint oil by supercritical carbon dioxide, J. Chem. Eng. Jpn. 26 (1993) 401–407, http://dx.doi.org/10.1252/jcej.26.401.
[25] B.C. Roy, M. Goto, T. Hirose, Extraction of ginger oil with supercritical carbon dioxide: experiments and modeling, Ind. Eng. Chem. Res. 35 (1996) 607–612, http://dx.doi.org/10.1021/ie950357p.
[26] H. Peker, M. Srinivasan, J. Smith, B. McCoy, Caffeine extraction rates from coffee beans with supercritical carbon dioxide, AIChE J. 38 (1992) 761–770, http://dx.doi.org/10.1002/aic.690380513.
[27] J. Tello, M. Viguera, L. Calvo, Extraction of caffeine from Robusta coffee (*Coffea canephora* var. Robusta) husks using supercritical carbon dioxide, J. Supercrit. Fluids 59 (2011) 53–60, http://dx.doi.org/10.1016/j.supflu.2011.07.018.
[28] M.R. Lee, C.Y. Lin, Z.G. Li, T.F. Tsai, Simultaneous analysis of antioxidants and preservatives in cosmetics by supercritical fluid extraction combined with liquid chromatography-mass spectrometry, J. Chromatogr. A. 1120 (2006) 244–251, http://dx.doi.org/10.1016/j.chroma.2006.01.075.
[29] S. Scalia, Determination of sunscreen agents in cosmetic products by supercritical fluid extraction and high-performance liquid chromatography, J. Chromatogr. A 870 (2000) 199–205.
[30] A. Weir, P. Westerhoff, L. Fabricius, N. von Goetz, Titanium dioxide nanoparticles in food and personal care products, Env. Sci Technol. 46 (2012) 2242–2250, http://dx.doi.org/10.1021/es204168d.
[31] J.M. Pettibone, D.M. Cwiertny, M. Scherer, V.H. Grassian, Adsorption of organic acids on TiO_2 nanoparticles: effects of ph, nanoparticle size, and nanoparticle aggregation, Langmuir 24 (2008) 6659–6667.
[32] Y.S. Choi, S. Nešić, Determining the corrosive potential of CO2 transport pipeline in high pCO2-water environments, Int. J. Greenhouse Gas Control. 5 (2011) 788–797, http://dx.doi.org/10.1016/j.ijggc.2010.11.008.